

PREDICTION OF MODE-I DELAMINATION GROWTH FOR THE MULTIDIRECTIONAL LAMINATES OF CFRP

Naoki. YAMAMOTO^{1*}, Takaomi. INADA¹, Takuya. SUZUKI¹

¹IHI Corporation, 1, Shin-Nakahara-Cho, Isogo-ku Yokohama 235-8501 Japan
*naoki_yamamoto@ihi.co.jp

Keywords: CFRP, Double Cantilever Beam Tests, Delamination, Virtual Crack Closure Techniques

ABSTRACT

Although estimating interlaminar fracture strength is a key issue in the design of composite structures, mode-I interlaminar fracture tests are generally conducted for only unidirectional laminates. Since multidirectional laminates are used in composite structures, an understanding of delamination characteristics and prediction techniques for the multidirectional laminates are needed. In this paper, the delamination growth simulations by VCCT(Virtual Crack Closure Techniques) for the DCB(Double Cantilever Beam) tests were conducted for the multidirectional laminates of CFRP. The starting points of delamination growth and the load-displacement curves corresponded closely with the DCB tests.

1 Introduction

Predicting the fracture strength of composite structures is a significant issue. However, owing to the existence of initial defects and the complex fracture mechanism, the structural strength can be proven by tests in most cases. It seems that the fracture mechanics using VCCT is a valid way to estimate the strength of composite structures, but the DCB tests, in order to measure the interlaminar fracture toughness, are not generally performed on multidirectional laminates.

The effect of the multidirectional laminates of CFRP was studied experimentally on the Mode-I interlaminar fracture toughness^[1], but the analytical research and prediction methods for the delamination were not investigated. The analytical studies using VCCT were conducted on the multidirectional laminates for estimating the starting point of delamination^{[2]-[4]}, but the delamination growth was not mentioned in these papers.

In this paper, the DCB tests were conducted on the multidirectional laminates of CFRP(Carbon Fiber Reinforced Plastics) , and the values of mode-I interlaminar fracture toughness, G_{IC} and G_{IR} , were calculated through the delamination growth. The fracture toughness at the delamination starting point, G_{IC} , was the smallest when the interlaminar angle was 0//0. In addition, delamination growth simulations by VCCT were performed on multidirectional DCB specimens. The load-displacement curves of simulation corresponded closely with the DCB test results. Furthermore the mesh size effect of VCCT was negligibly small for the energy release rate G_I .

2 DCB Tests

2.1 Specimens

DCB test specimens of CFRP (T700SC/#2592, Toray Industry, Inc.; product name 3252S-12) were used. The shape and dimensions of the DCB specimens are shown in Figure 1. For the

implementation of initial delamination, a two-ply Kapton film of 12.5- μm thickness was inserted in a neutral laminate surface. The stacking sequence of each specimen is shown in Table 1. Interlaminar fiber angles on the neutral laminate surface are 0//0, 0//90, and 45//−45. The number of test specimens is 3 for the 0//0 interface, and 5 for the 0//90 and 45//−45 interfaces.

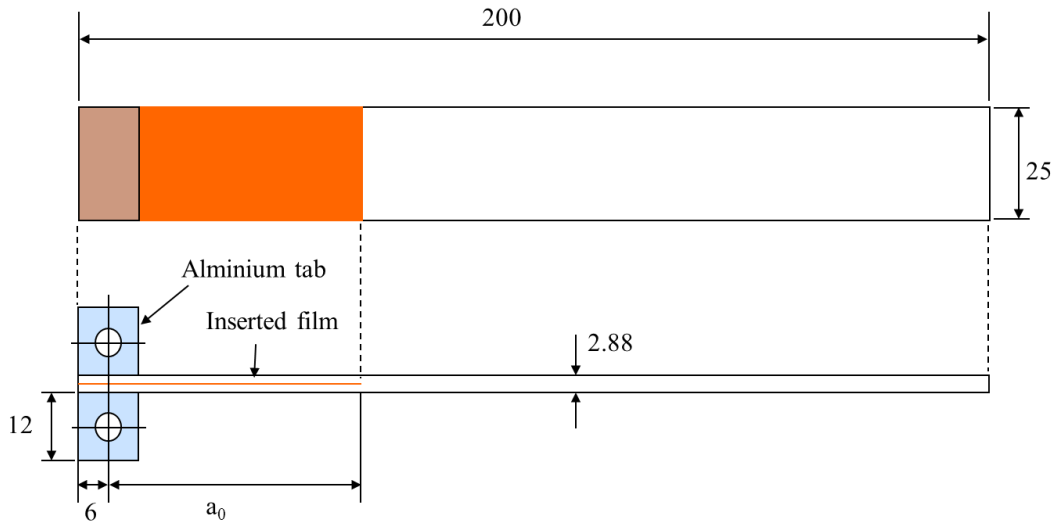


Figure 1. DCB test specimen

Fiber angles at interface	Stacking sequence
0//0	[0 ₁₂ //0 ₁₂]
0//90	[0 ₉ / 90 ₃ //0 ₃ /90 ₃ /0 ₆]
45//−45	[45/−45/0 ₈ /−45/45 //−45/45/0 ₈ /45/−45]

Table 1. Stacking sequence

2.2 Test Methods

Shimazu 100 kN test equipment was used for the DCB tests. Tensile load was given through the aluminum tabs bonded at the end of the specimen until delamination growth reached 70 mm. DCB test configuration is shown in Figure 2. All tests were performed at a cross-head speed of 2-3 mm/min. Delamination growth length was recorded at approximately every 10 mm.

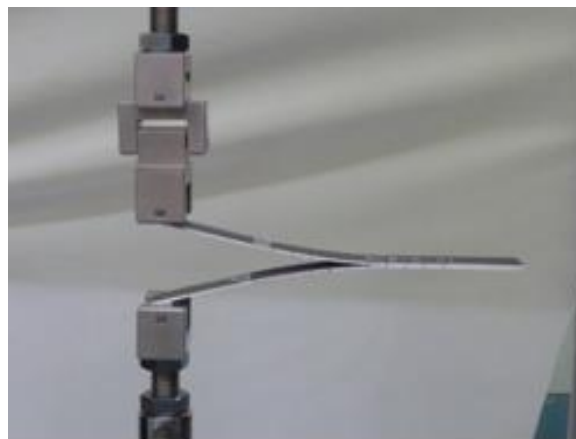


Figure 2. DCB test configuration

2.2 Test results and consideration

Using the data derived from the DCB tests, the values of the Mode-I interlaminar fracture toughness at the starting point of delamination, G_{IC} , and the Mode-I interlaminar fracture toughness through delamination, G_{IR} , were calculated by the modified compliance calibration method^[5] as equations(1) and (2). In these equations, α_1 was derived from equation (3), which was linearized approximately by plotting $a/2H$ and $(B\lambda)^{1/3}$.

$$G_{IC} = \frac{3}{2(2H)} \left(\frac{P_c}{B} \right)^2 \frac{(B\lambda_0)^{2/3}}{\alpha_1} \quad (1)$$

$$G_{IR} = \frac{3}{2(2H)} \left(\frac{P}{B} \right)^2 \frac{(B\lambda)^{2/3}}{\alpha_1} \quad (2)$$

$$\frac{a}{2H} = \alpha_1 (B\lambda)^{1/3} + \alpha_0 \quad (3)$$

where $2H$ is the thickness of the specimen[mm], B is the width of the specimen [mm], λ_0 is the initial elastic compliance on the load-displacement curves[mm/N], λ is the elastic compliance on the load-displacement curves[mm/N], P is the load[N], and P_c is the load at the starting point of delamination[mm] .

The average values of G_{IC} of each stacking sequence are shown in Table 2. The G_{IC} was the smallest in the case of the 0//0 interface and the largest in the case of the 45//-45 interface. It seems that the delamination growth was prevented if the propagation direction differed from the fiber direction at the interface.

R-curves of each test results and the test average for each stacking sequence are shown in Figures 3-5. In the case of the 0//0 and 0//90 interfaces, the fracture toughness increased uniformly. On the other hand, in the case of the 45//-45 interface, the fracture toughness fluctuated. To investigate the differences, the specimens were split into two pieces at the neutral surface after the tests. In the case of the 45//-45 interface, two different delamination patterns were observed. One propagated into the 45° laminates (Figure 6) which corresponds to Case-A of Figure 5. R-curves were relatively smooth. The other propagated both into the 45° laminates and along the 45//-45 interface(Figure 7) and corresponds to Case-B of Figure 5.

Interlaminar angles	G_{IC} [kJ/m ²]	
	(Coefficient of variation %)	
0//0	0.300	(5.3)
0//90	0.412	(9.4)
45//-45	0.530	(9.3)

Table 2. Summary of G_{IC}

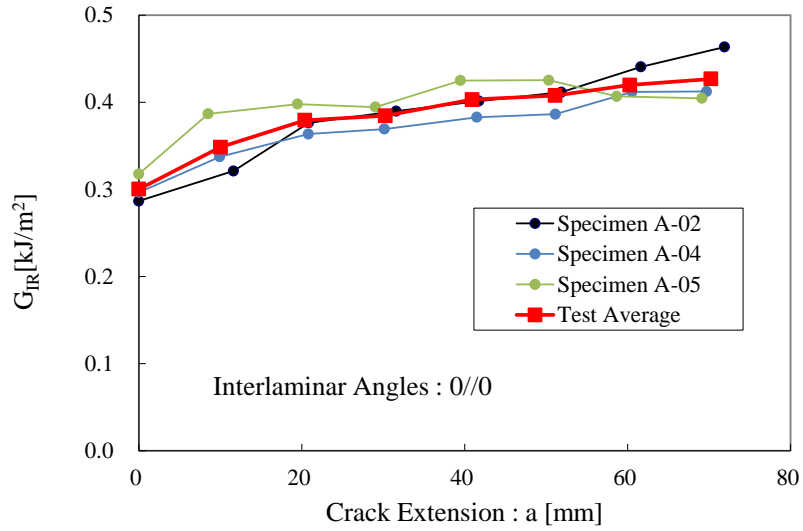


Figure 3. R-curves of 0//0 interfaces

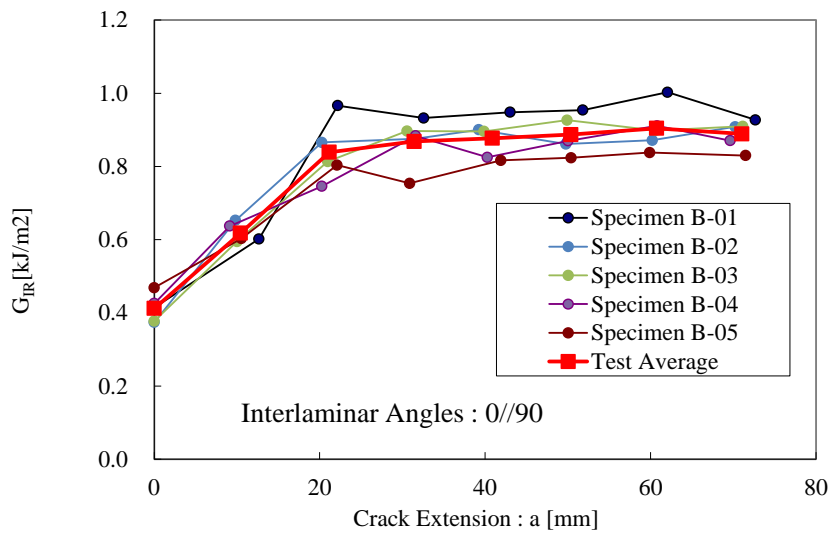


Figure 4. R-curves of 0//90 interfaces

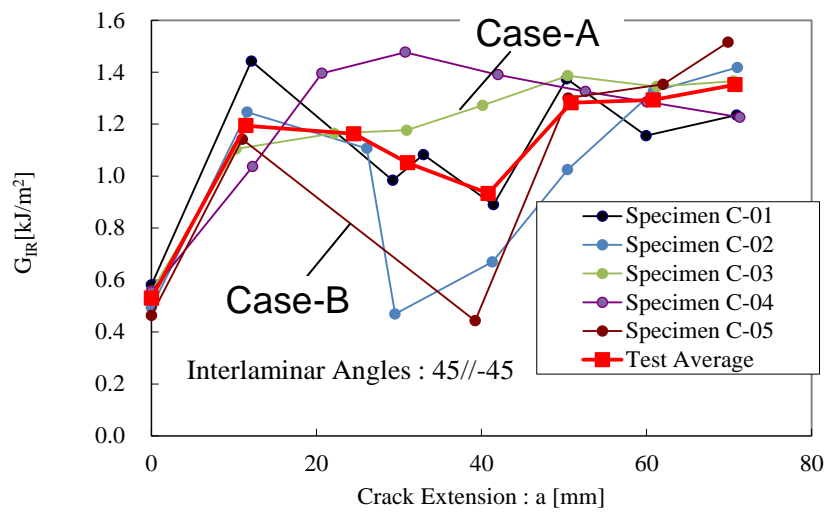


Figure 5. R-curves of 45// -45 interfaces

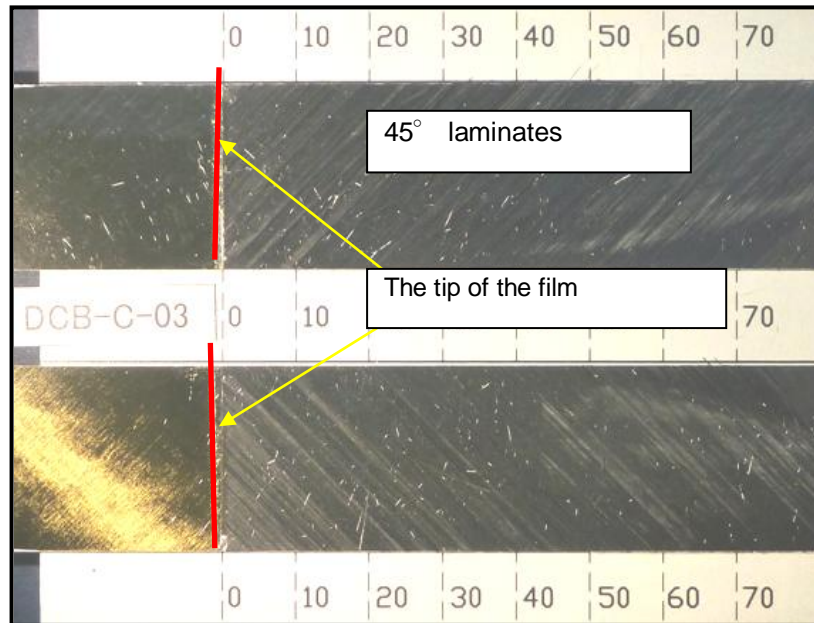


Figure 6. Interlaminar fracture behavior (45//45) (Case-A)

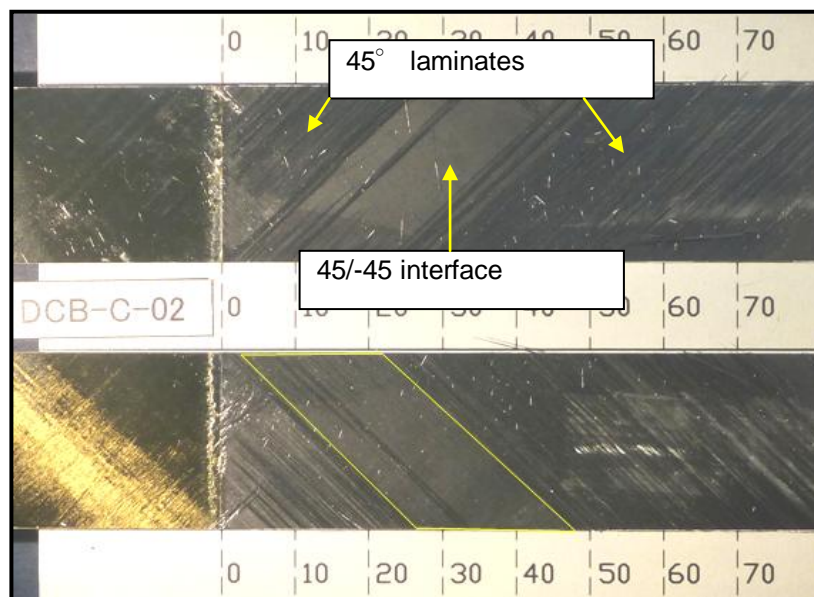


Figure 7. Interlaminar fracture behavior (45//45) (Case-B)

3 Delamination growth simulations by VCCT

3.1 Analytical Methods

Delamination growth simulations by VCCT were conducted for the 0//0, 0//90 and 45//45 interfaces. The analysis model is shown in Figure 8. 4 node plane strain elements were used. The mesh size was 0.5 mm in length and had a thickness of 0.12 mm (1 ply). In addition, in order to examine the mesh size dependence, analysis for the 1.0mm mesh length was also performed. At the interfaces of delamination, the contact areas were considered. ABAQUS6.11-1 was used for numerical analysis. Material constants are shown in Table 3.

At the bottom of the load point a simple support condition was imposed, and at the top of the load point, the displacement was given. Geometric nonlinearity was considered in the analysis.

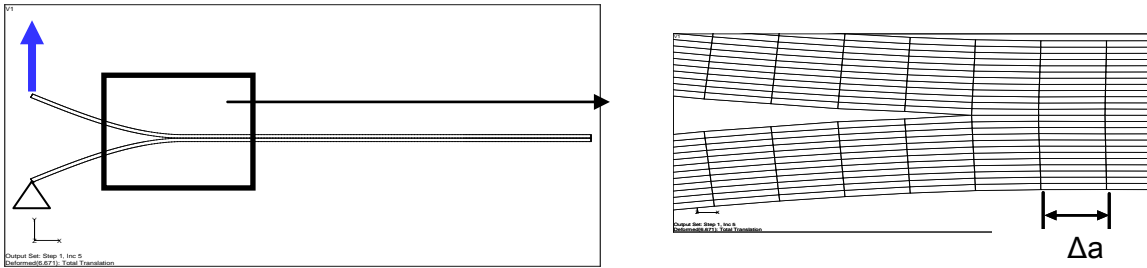


Figure 8. Analytical model

E_1 [MPa]	E_2 [MPa]	E_3 [MPa]	ν_{12}	ν_{13}	ν_{23}	G_{12} [MPa]	G_{13} [MPa]	G_{23} [MPa]
101248	9380	9380	0.27	0.27	0.39	4280	4280	3374

(Note: Subscript 1,2,3 indicate fiber direction, perpendicular direction to fiber, and thickness respectively.)

Table 3. Material data

The Mode-I energy release rate, G_I , was derived by VCCT in accordance with equation (4). In the equation W and Δa indicate the width of the specimen and the mesh length respectively. The symbol f_p and δ_p' are defined^[6], as shown in Figure 9.

$$G_I = \frac{1}{2W\Delta a} f_p \delta_p' \quad (4)$$

$$G_I \geq G_{IR} \quad (5)$$

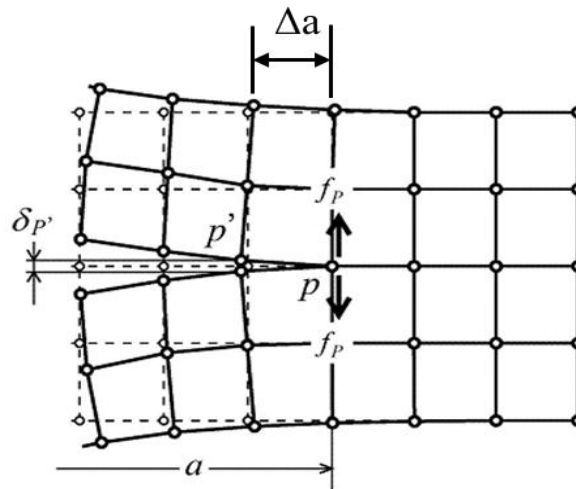


Figure 9. Schematic view of VCCT

3.2 Analytical Results

The load-displacement curves of each test results and analytical results are shown in Figures 10-12. The delamination growth simulations corresponded closely with the test results, especially in the case of the 0/0 and 0/90 interfaces. In the case of the 45/-45 interface, the numerical results corresponded with the test results just before the starting point of the delamination growth and after the propagation was large enough. In the same figures, the analytical results of the 1.0 mm mesh length were plotted. The mesh size effect was negligibly small. The loads at the starting point of delamination growth are shown in Table 4 for the test results and the simulations. Both results corresponded closely.

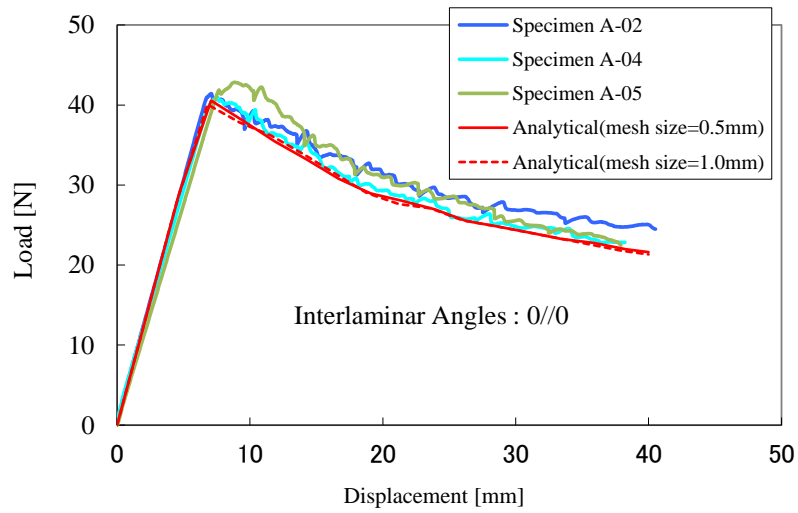


Figure 10. Load-Displacement curves of 0//0 interfaces

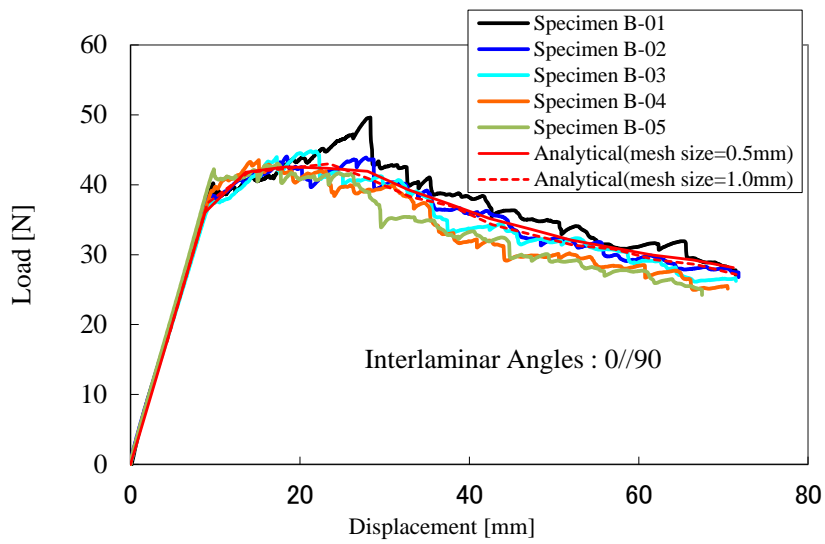


Figure 11. Load-Displacement curves of 0//90 interfaces

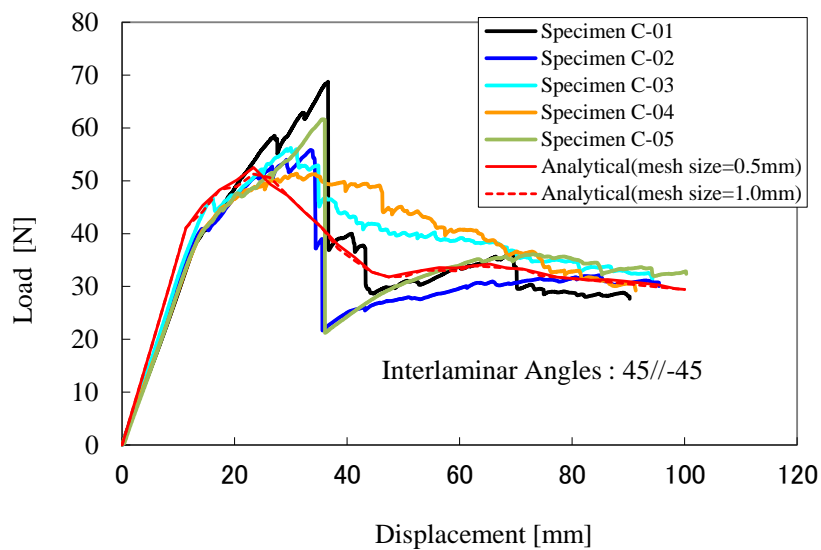


Figure 12. Load-Displacement curves of 45//-45 interfaces

Interlaminar angles	Test average [N]	Analytical [N]	
		Mesh size : 0.5mm	Mesh size : 1.0mm
0//0	41.4	40.7	40.1
0//90	39.7	40.9	39.2
45//45	40.4	41.0	40.9

Table 4. Load at starting point of delamination growth

4 Conclusions

- (1) The DCB tests were performed on the multidirectional laminates of CFRP whose interfaces were 0//0, 0//90 and 45//45 and the values of the interlaminar fracture toughness were calculated through the delamination growth. The G_{IC} was the smallest in the case of the 0//0 interface and the largest in the case of the 45//45 interface. In the case of the 0//0 and 0//90 interfaces, the fracture toughness increased uniformly. On the other hand, in the case of 45//45 interface, the fracture toughness fluctuated because of two different delamination patterns.
- (2) The delamination growth simulations by VCCT for the DCB tests were conducted for the 0//0, 0//90 and 45//45 interfaces. The load of the starting points of delamination growth and the load-displacement curves corresponded closely with the DCB tests. The longitudinal mesh size effect was negligibly small for the Mode-I energy release rate G_I .

References

- [1] Cho, I., Kimpara, I., Kageyama, K., Ohsawa, I., Effect of Fiber Orientation on the Mode I Interlaminar Fracture Behavior of CF/EPOXI Laminates, *J. Soc. Mat. Sci., Japan*, Vol.41, No.467, pp.1292-1298(1992) (in Japanese)
- [2] Morais, A.B., Moura, M.F., Marques, A.T., Castro, P.T., Mode-I interlaminar fracture of carbon/epoxy cross-ply composites, *Composites Science and Technology*, Vol.62, pp.679-686(2002)
- [3] Morais, A.B., Double cantilever beam testing of multidirectional laminates, *Composites : Part A*, Vol. 34, pp.1135-1142(2003)
- [4] Pereira, A.B., Morais, A.B., Mode I interlaminar fracture of carbon/epoxy multidirectional laminates, *Composites Science and Technology*, Vol.64, pp. 2261-2270(2004)
- [5] JIS K 7086, *Testing methods for interlaminar fracture toughness of carbon reinforced plastics*(2012) (in Japanese)
- [6] Ben, G., Ishikawa, R., *The composite engineering*, Baihukan (2005) (in Japanese)